Supplementary information

Enhancing UV photodetection performance of an individual ZnO microwire p-n homojunction via interfacial engineering

Kai Tang,[a] Mingming Jiang,*[a] Bingwang Yang,[a] Tong Xu,[a] Zeng Liu,[b] Peng Wan,[a] Caixia Kan,[a] and Daning Shi*[a]

[a] College of Physics, MIIT Key Laboratory of Aerospace Information Materials and Physics, Key Laboratory for Intelligent Nano Materials and Devices, Nanjing University of Aeronautics and Astronautics, No. 29 Jiangjun Road, Nanjing 211106, China;
*E-mail: mmjiang@nuaa.edu.cn; shi@nuaa.edu.cn
[b] Innovation Center for Gallium Oxide Semiconductor (IC-GAO), College of Integrated Circuit Science and Engineering, Nanjing University of Posts and Telecommunications, Nanjing 210023, China.

Table 1 The electrical transport properties of ZnO:Sb MW and ZnO film.

Category	**Mobility ($cm^2V^{-1}s^{-1}$)**	**Carrier concentration (cm^{-3})**
ZnO:Sb MW	2.6	5.4×10^{17}
ZnO film	5.0	1.0×10^{19}

Theoretical distribution width of depletion regions.[1]

The theoretical distribution width of depletion in p-ZnO:Sb region ($w_{ZnO:Sb}$) and in n-ZnO region (w_{ZnO}) can be evaluated through the formula:

$$w_{ZnO} = \sqrt{\frac{2\varepsilon_{ZnO}\varepsilon_0 n_{ZnO:Sb} V_{in}}{e n_{ZnO}\left(n_{ZnO} + n_{ZnO:Sb}\right)}} \tag{1}$$

$$w_{ZnO:Sb} = \sqrt{\frac{2\varepsilon_{ZnO}\varepsilon_0 n_{ZnO} V_{in}}{e n_{ZnO:Sb}\left(n_{ZnO} + n_{ZnO:Sb}\right)}} \tag{2}$$

Where ε_{ZnO} is relative dielectric constants of ZnO (~8). $n_{ZnO:Sb}$ (~5.4×10^{17}) and n_{ZnO} (~1.0×10^{19}) are carrier concentrations. V_{in} is the built-in voltage (~2.0 V), ε_0 is the permittivity of vacuum, and e is elementary charge. From (1) and (2), w_{ZnO} is calculated as 3.0 nm, and $w_{ZnO:Sb}$ is calculated as 55.8 nm.

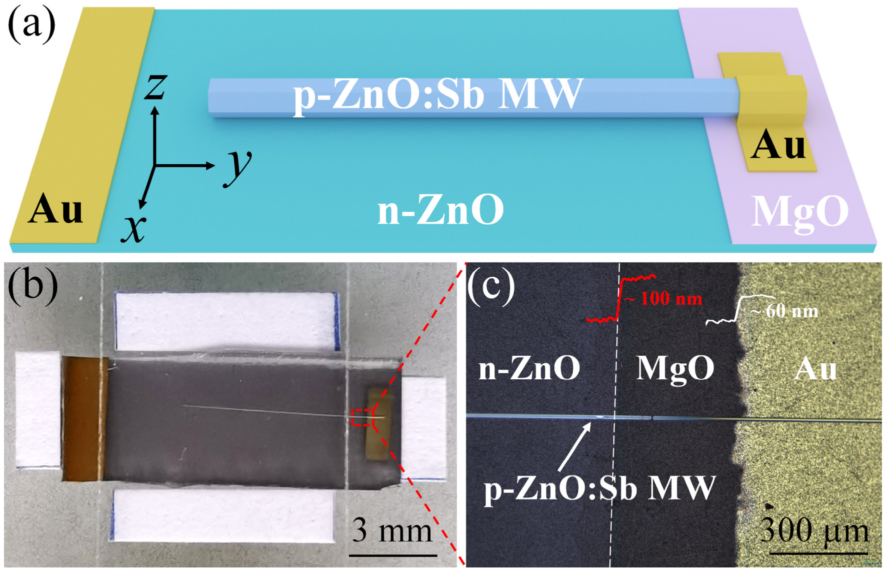

Figure S1. Schematic architecture of the as-designed p-ZnO:Sb MW/n-ZnO film homojunction photodetection device. (b) Optical photography of the as-designed p-ZnO:Sb MW/n-ZnO film homojunction photodetection device. (c) Enlarged view of the selected area.

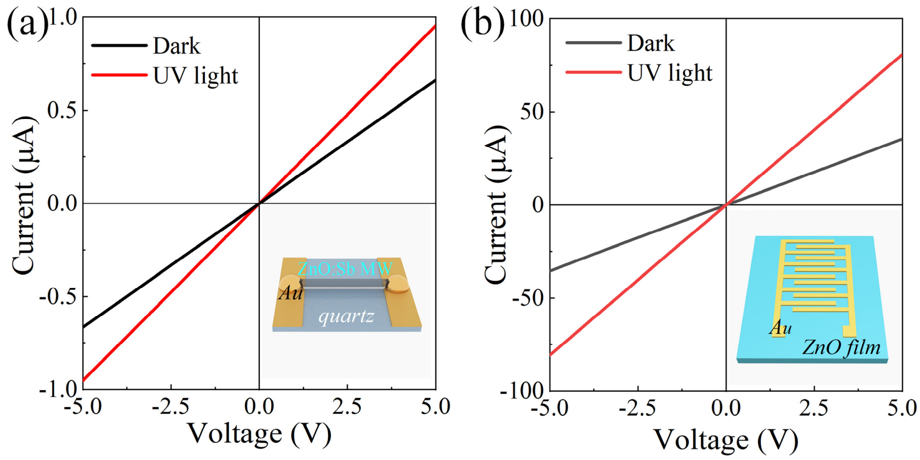

Figure S2. (a) *I-V* characteristic curves of Au-ZnO:Sb MW contact under dark and UV illumination. (b) *I-V* characteristic curves of ZnO film structure with Au interdigital electrodes under dark and UV illumination.

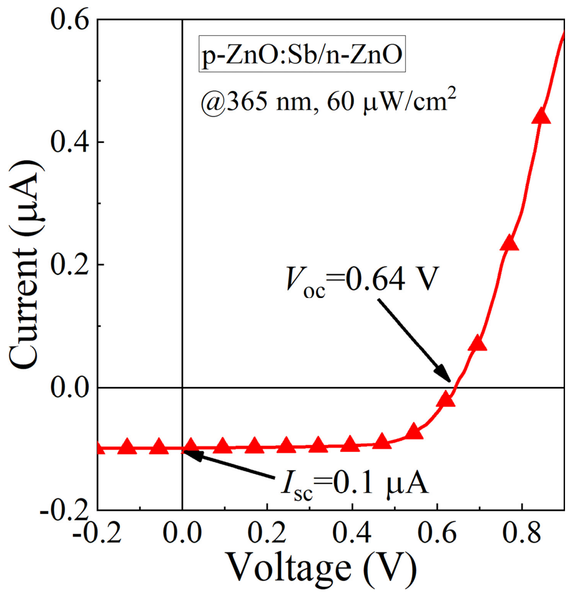

Figure S3. The *I-V* characteristic curve of a p-ZnO:Sb MW/n-ZnO homojunction PD under 365 nm illumination (~ 60 μW/cm^2).

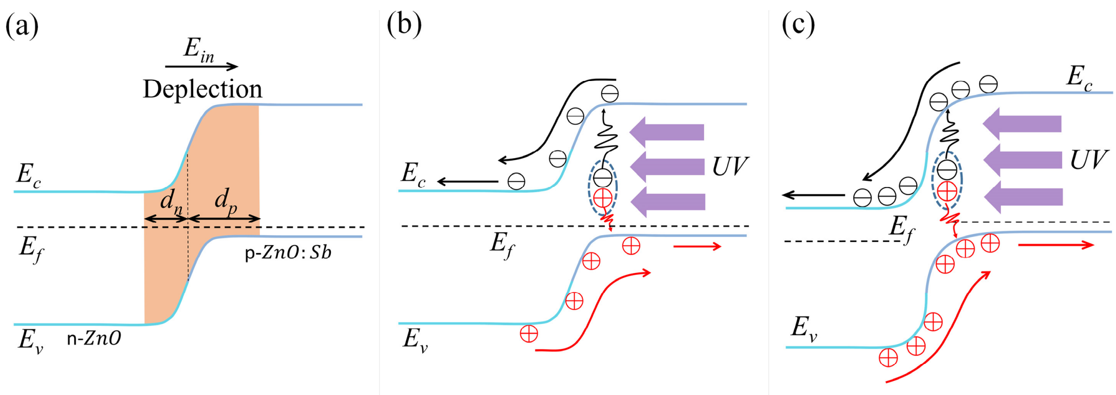

Figure S4. Energy band structure diagram of p-ZnO:Sb MW/n-ZnO homojunction PD. (a) under thermal equilibrium at zero bias; (b) under 365 nm illumination at zero bias; (c) under 365 nm illumination at a reverse bias.

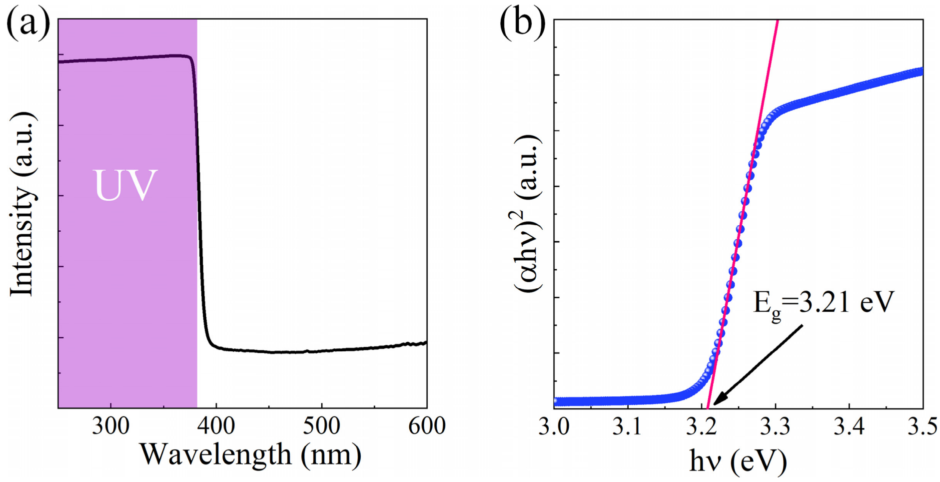

Figure S5. (a) Absorption spectra of single ZnO:Sb MW. (b) The corresponding optical bandgap of ZnO:Sb MW.

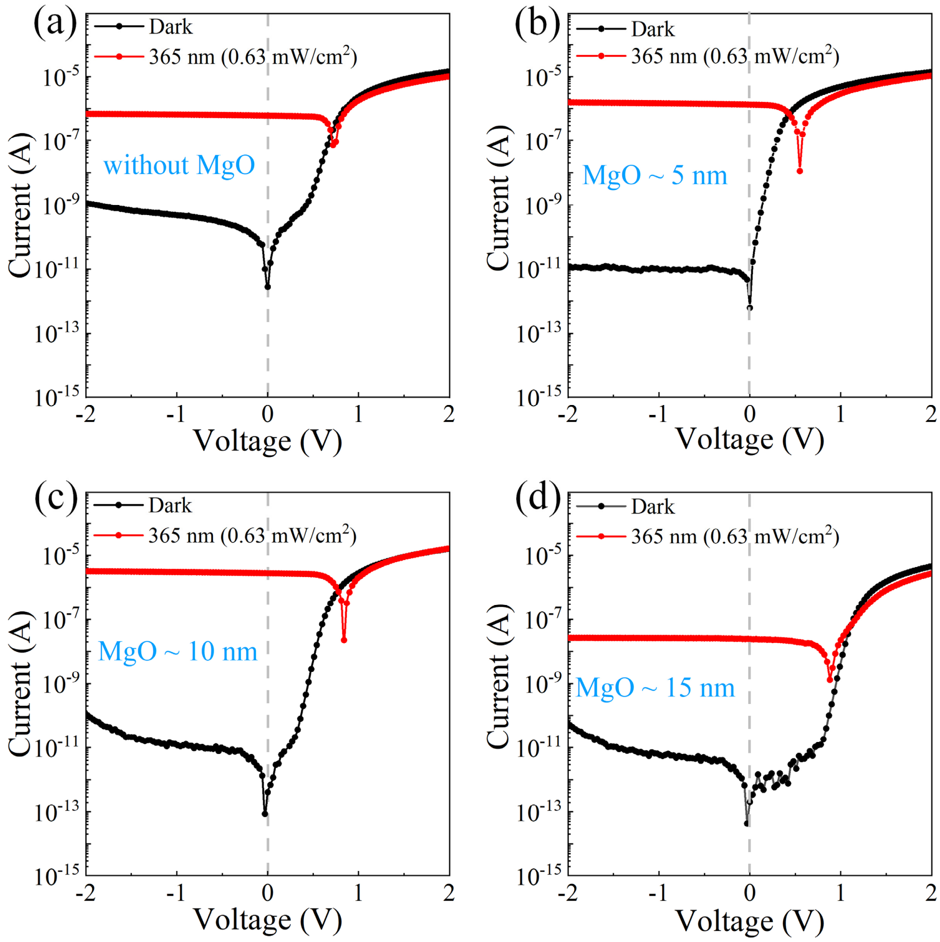

Figure S6. By varying the thickness of the inserted MgO interlayer, logarithmic *I-V* curves of as-constructed p-ZnO:Sb MW/i-MgO/n-ZnO homojunction PDs in darkness and 365 nm light illumination. (a) without MgO; (b) 5 nm MgO; (c) 10 nm MgO; (d) 15 nm MgO.

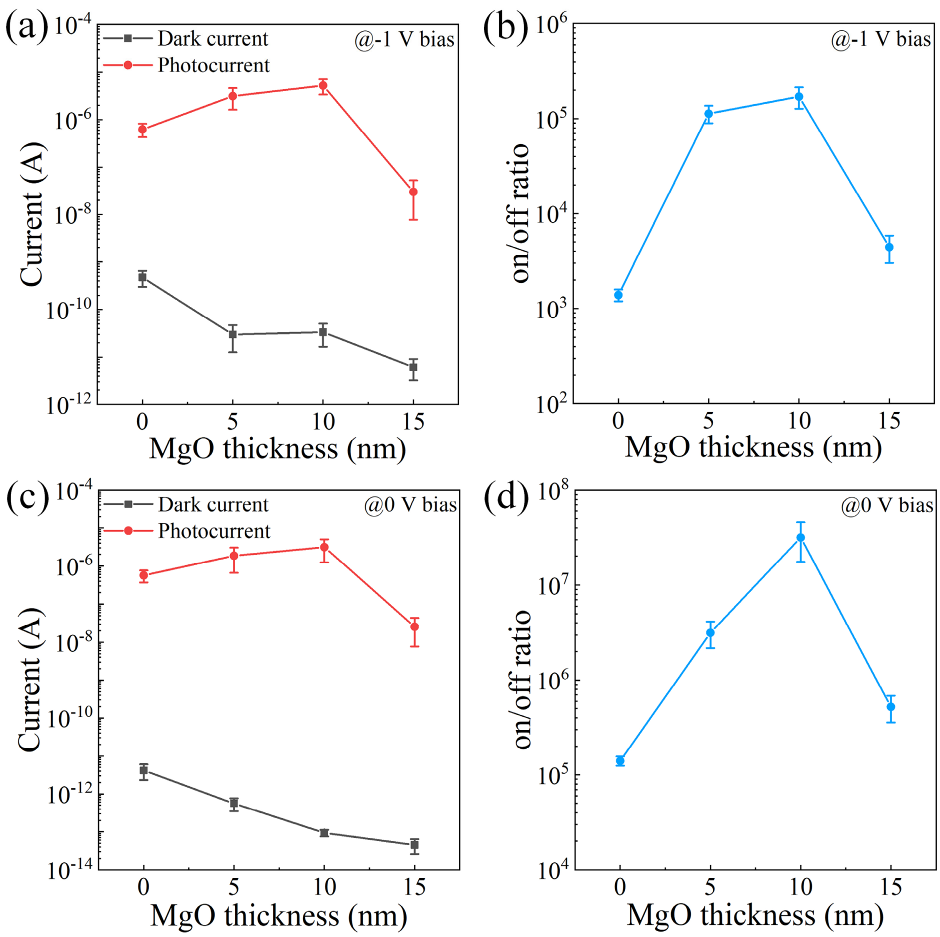

Figure S7. (a) The relationship between photocurrent, dark current and MgO thickness of as-constructed p-ZnO:Sb MW/i-MgO/n-ZnO homojunction PDs at -1V bias; (b) The relationship between on/off ratio and MgO thickness of as-constructed p-ZnO:Sb MW/i-MgO/n-ZnO homojunction PDs at -1V bias; (c) The relationship between photocurrent, dark current and MgO thickness of as-constructed p-ZnO:Sb MW/i-MgO/n-ZnO homojunction PDs at 0 V bias; (d) The relationship between on/off ratio and MgO thickness of as-constructed p-ZnO:Sb MW/i-MgO/n-ZnO homojunction PDs at 0 V bias.

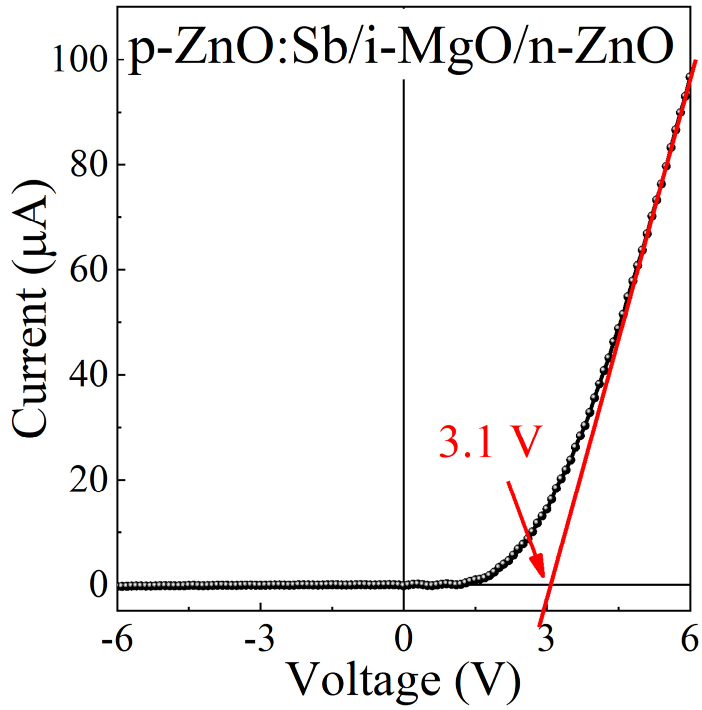

Figure S8. The *I-V* characteristic curve of a p-ZnO:Sb MW/i-MgO/n-ZnO homojunction PD in darkness.

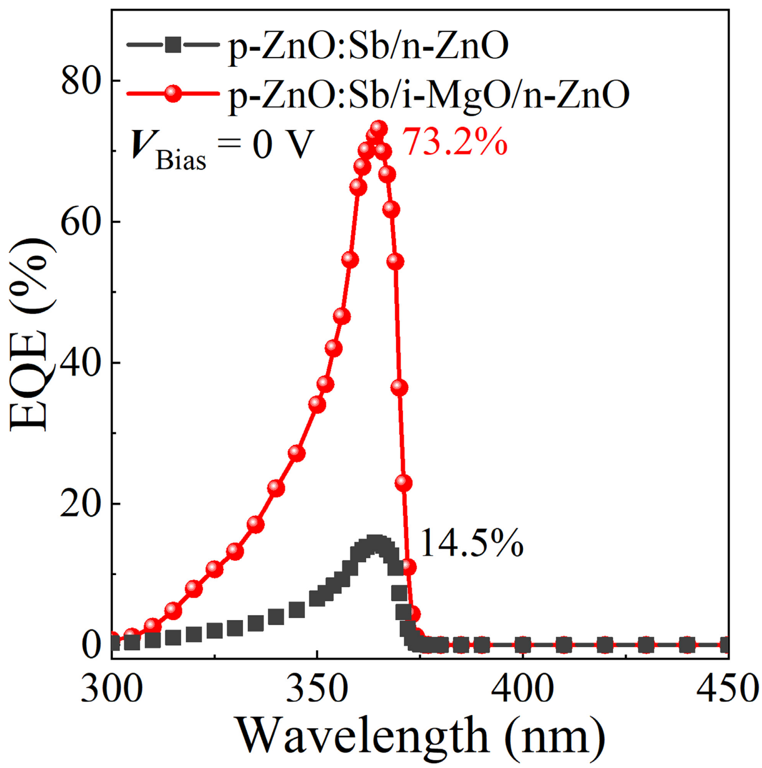

Figure S9. Comparison of the calculated EQE of the fabricated homojunction devices without applied bias.

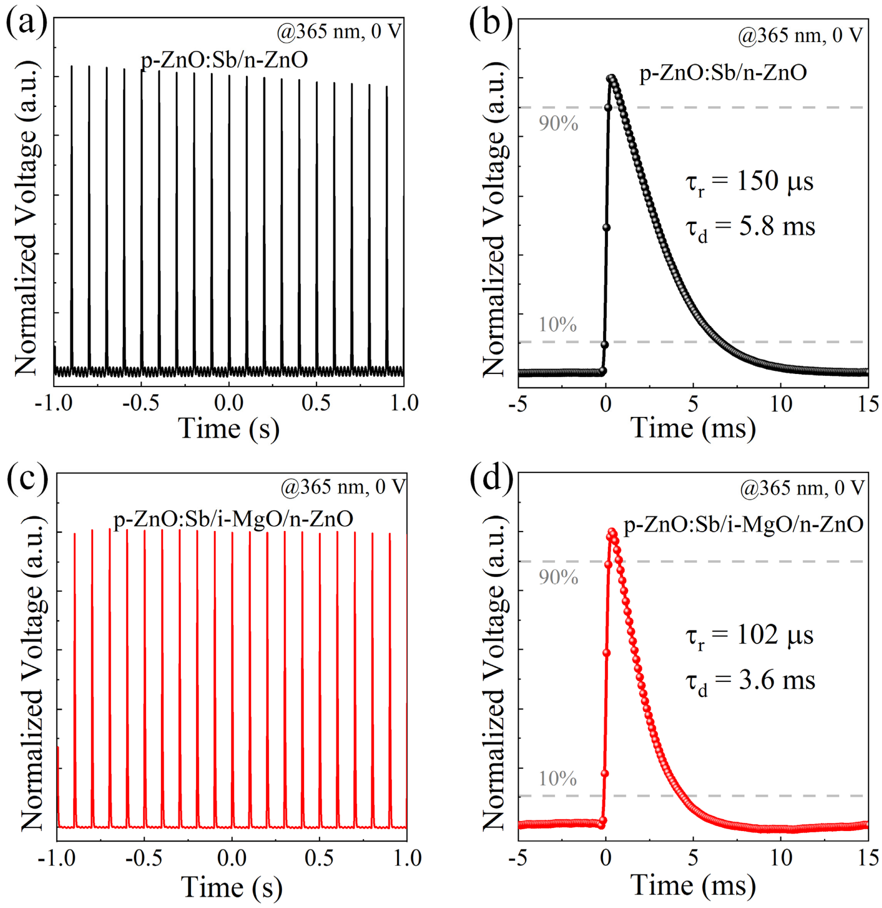

Figure S10 (a) Transient photoresponse of the p-ZnO:Sb MW/n-ZnO PD under 365 nm pulse laser illumination at the bias of 0 V. (b) Single period of the pulse response of the p-ZnO:Sb MW/n-ZnO PD. (c) Transient photoresponse of the p-ZnO:Sb MW/i-MgO/n-ZnO PD at 0 V bias under 365 nm pulse laser illumination at the bias of 0 V. (d) Single period of the pulse response of the p-ZnO:Sb MW/i-MgO/n-ZnO PD.

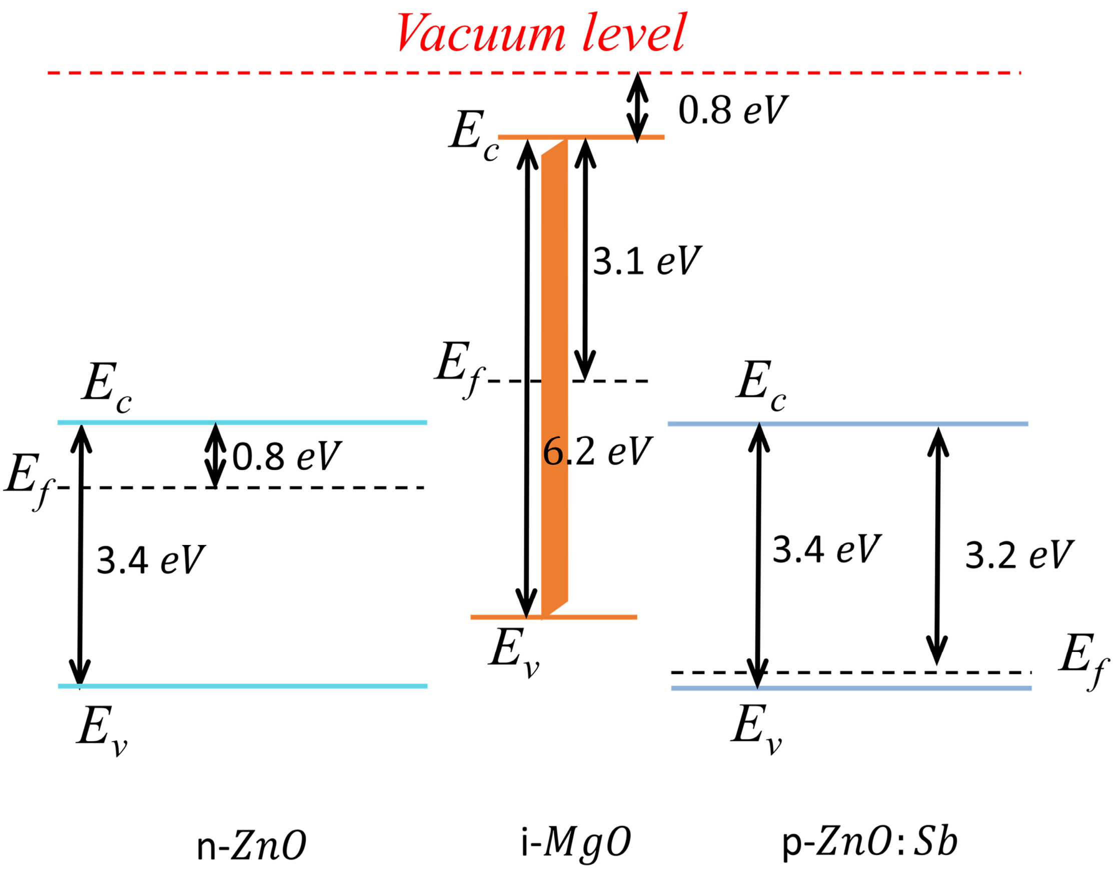

Figure S11. The energy band diagrams of p-ZnO:Sb, i-MgO[2-4] and n-ZnO before contact.

The stability of the fabricated p-ZnO:Sb MW/MgO/n-ZnO homojunction photodetector is critical to meet real-world applications. In general, the stability of photodetectors can be divided into their photostability and long-term stability. First, photostability is evident from the transient switching response of the as-constructed homojunction photodetector. The photoswitching responses were recorded for a constant operation at zero bias under 365 nm light illumination with an optical power intensity of 2.5 mW/cm^2. As illustrated in Figure S12(a), the detector exhibits stable and reproducible ON/OFF behavior over 400 consecutive cycles, especially for electrically stable features. Subsequently, the as-prepared p-ZnO:Sb MW/MgO/n-ZnO homojunction photodetector was kept in an air environment with 50% humidity for about 100 days, while without any encapsulation and protection. During the stored procedure, we conducted a stability measurement of the fabricated photodetector, observing its photoswitching responses when measured at 0 V under 365 nm illumination via light power intensity ~2.5 mW/cm^2. The measured time-domain response of the device over a series of ON/OFF switching cycle, as seen in Figure S12(b). It suggests that the photodetector maintained a good electrical stability. The experimental results suggest that the proposed photodetector is suitable for long-term, highly reliable ultraviolet photodetection.

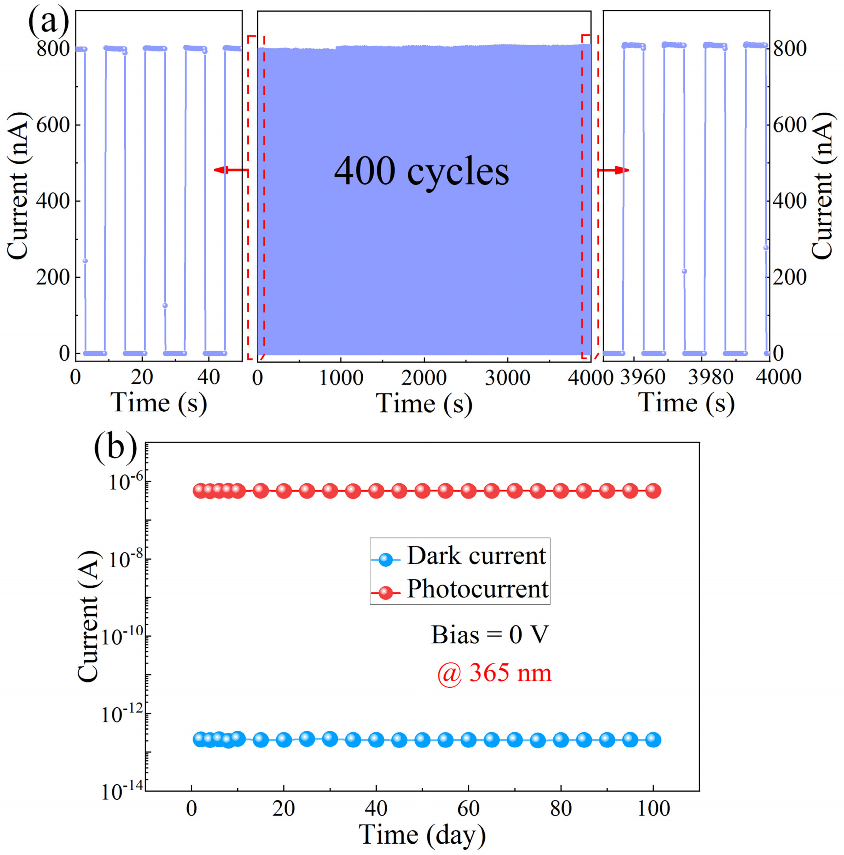

Figure S12. Photostability and long-term stability measurement of our p-ZnO:Sb MW/MgO/n-ZnO homojunction photodetector. (a) 400 cycles of transient photoresponse curve of the fabricated photodetector under 365 nm light illumination of 2.5 mW/cm^2 in a self-powered manner. Inset: Enlarged 4 cycles photoresponse curves. (b) Long-term test of the photoswitching features of the fabricated device (~ 100 days).

References

1. Wan, P., et al., *Doping Concentration Influenced Pyro-Phototronic Effect in Self-Powered Photodetector Based on Ga-Incorporated ZnO Microwire/p+-GaN Heterojunction.* Advanced Optical Materials, 2021. **10**(2).
2. Kumar, A. and J. Kumar, *On the synthesis and optical absorption studies of nano-size magnesium oxide powder.* Journal of Physics and Chemistry of Solids, 2008. **69**(11): p. 2764-2772.
3. Badar, N., et al., *Band Gap Energies of Magnesium Oxide Nanomaterials Synthesized by the Sol-Gel Method.* Advanced Materials Research, 2012. **545**: p. 157-160.
4. Ismail, R.A., et al., *Preparation of low cost n-ZnO/MgO/p-Si heterojunction photodetector by laser ablation in liquid and spray pyrolysis.* Materials Research Express, 2018. **5**(5).